Journal of Science and Technology
ISSN: 2456-5660 Volume 5, Issue 6, Nov-December 2020

www.jst.org.in *DOI: https://doi.org/10.46243/jst.2020.v5.i6.pp128-140*

Simulation of Quasi-Isotropic E-Glass Composite Laminate at Low Velocity Impact with Cohesive Interface Elements

Enock A. Duodu

Department of Mechanical Technology Education, University of Education, Winneba- Ghana
Corresponding Author: eaduodu@uew.edu.gh

To Cite this Article

Enock A. Duodu, "Simulation of Quasi-Isotropic E-Glass Composite Laminate at Low Velocity Impact with Cohesive Interface Elements", Journal of Science and Technology, Vol. 05, Issue 06, Nov-December 2020, pp128-140

Article Info

Received: 10-07-2020 Revised: 16-10-2020 Accepted: 22-10-2020 Published: 25-10-2020

Abstract: *This paper examines the expediency of interface elements in modeling of impact damage analysis for E-glass composite laminate under low velocity impact test. Numerical modelsare built adopting cohesive interface behavior to authenticate the cross-ply damage response; and successively used the strategy to model the impact response of quasi-isotropic composite laminate. Impact test are performed to characterize the induced-damage behavior in quasi-isotropic composite laminate at different impact energy test in terms of impact force, displacement and damage size as well as the stress failure trajectory. Numerical result shows reliability of the model for structural impact analysisin damage initiation and progression in laminated composite plates. The simulation result though reveals large deformation, yet, did not yield in total fracture. This development shows the importance of adopting interface elements in structural impact damage criterion to trigger constraints effect on initiation phase.The study also reveals that the bottom most surface suffers huge deformation compare to the impact surface. It divulges that the extent of damage area in each ply of the composite laminate orients in the fiber direction in 'star-shaped contour. The main novelty is the capability of using this model for structural impact analysis on both cross-ply and quasi-isotropic composite laminate.*

Keywords*: Cohesive interface element; delamination; low-mass; simulation model; structural stiffness*

I. Introduction

In recent times, composite have replaced metallic materials in the construction of structures such as inaerospace, marine, civil and automotive fields due to their high specific strength, light weight and long service life. Composites are believed to have superior potential utilization as the main load-bearing structure in many industries. However, these materials are poor to impact resistance owing to loading conditions, which results in fragile behavior and damage resistance. Impact damage deformation in composite laminates at low impact test is critical phenomenon, especially in the application of aircraft structures.Failure of composite material is a multifaceted process encompassing intra-laminar and inter-laminar damages which results in reduction of stiffness and strength properties under loading. Therefore, knowing the fundamental mechanisms that account for failure is vital in order to improve the mechanical properties of the composite materials.

Generally,composite laminates under impact loading becomes very complex to analyze and therefore necessitates the application of an efficient modelling tool to predict accurate impactresponse of intra-laminar and inter-laminar failures.Owing to this phenomenon, mostresearchers have adopted two main techniques including virtual crack closure-integral technique (VCCT) and cohesive zone model (CZM)to predict delamination in composite laminates. The CZMis based oninterface elements whilstVCCT uses the fracture mechanics concept.

Today, numerous studies on impact behavior of composite laminates are found inliterature. Choi et al. [1]formulated displacement field plate theory to investigate low velocity impact behavior of composite laminates under in-plane loads. It reveals that impact loads and damage areascompare well with experimental test at all the energy test levels. Xiao et al.[2]carried out analytical formulation to estimate the damage area of composite laminates induced with low velocity impact.It establishes that the ultimate contact force and initial inter-laminar shear strength

based on Eshelby'sequivalencedefinition agrees well empirical data. Olsson [3] proposed a model to calculate the crackinitiation and growth during quasi-static response with large mass impactors and reveals that theresidual bending stiffness degradationis effective to all layups and boundary conditions.Hosur et al. [4] carried out experimental study to analyze the behavior of different shades of composites subjected to low velocity impact loading.It found that the hybrid composites are slightly stiffer than glass/epoxy and carbon/epoxy laminates.

Again, Zhang et al. [5] have applied practical test to analyze large mass impact in three shades of composite laminates.Itdiscloses that the effect of single-layer fabric structure exhibits better impact performance, and delamination resistance compares with other composites.Sevkat et al.[6]carried out empirical studieson hybrid reinforced composite laminates and presentsthat impact behavior of the composite is considerably inhibited by the nylon/basalt fiber content.Similarly, test investigation of large mass impact test ontransverse woven carbon composite is performed[7]. The study disclosesthat MWCNTs enhance impact trajectory and limitthe damage size in the woven carbon fiber composites. Mitrevski et al.[8] have experimentally analyzed the effect of impactor shape and tensile biaxial impact loading on thin glass fiber reinforced polyester laminated composite;and noticed that the contact force, impact energy and damage area remains the same during loading conditions.

Recently, many numerical impact assessments on composite laminateshave been accomplished.Lopes et al. [9, 10] have used experimental and simulation to analyze damage of multi-directional ply composite laminate at low velocity impact. The study divulges that largest delamination damage emerges at the innermost interface which results in decline of composite laminate residual strength. Zhang et al. [11] employed simulation model to analyze large mass impact damage test on composite laminate where cohesive elements are introduced in the formulation. The report shows importance of Hashin failure criterion in the model triggerfiber breaking, matrix failure and fiber-matrix debonding. Equally,Aymerich et al. [12]have numerically analyzed the structural behavior of composite laminate with cohesive element at low velocity impact, and presented accurate prediction of the structural behavior at different impact test levels.

Most recently, Ghoushji[13] investigates the potentials in natural ramie/bio-epoxy composite in crash energy absorption applications. The results indicated that natural ramie/bio-epoxy composite tube has the great potential to be used as an effective energy-absorbing device. El-baky[14]employs statistical analysis to analyze the impact response of hybrid laminated composites to know their suitability and adaptability for different industrial applications. Zeleniakiene[15, 16]analyzed the possibility of finite element modelling by homogenization approach for elastomeric polychloroprene/versatic acid vinyl ester/methyl methacrylate/2-ethylhexyl acrylate copolymer blend.Safi[17, 18] evaluated the effect of interface modification on the interfacial adhesion and tensile properties of glass fabric/epoxy composites in two directions, where the integration of colloidal silica into the hybrid sizing dramatically modified the fiber surface texture and created mechanical interlocking between the glass fabric and resin.

Even though, some numericalinvestigationsare highlighted to enhance the interfaceframework of composites[19-21],yet further studies on E-glass/epoxy are crucial for their effective utilization in the aviation industry.In this study, surface-based cohesive contact model is adopted for inter-laminar analysis due to the advantage ofpredicting initiation and evolution without previous knowledge of crack location and propagation direction.A 3D quasi-isotropic numerical model is developed toanalyze damage characteristics of composite plate.The present model is then executed into ABAQUS/Explicit 6.11 version platform via a user-defined subroutine VUMAT, written in FORTRAN.Numerical analysisof the model is deliberated in detail further comparesto experimental data in referencewith respect to time histories of impact force and displacement in addition to damage envelope sizes. The numerical predictions were found to be in acceptable agreement with the experimental data to validate the efficiency and dependability of the proposed finite element model.

II. Damage Modeling

Intra-laminar Damage

The in-plydamage model is based on CDM where internal state variables are used as coefficients to trigger in-ply damage development in order to degrade the material stiffness.Failure modes are formulated and applied into ABAQUS/Explicit solver through the user-defined subroutine.This environment allowsexamining the modes of fibertensile failure,fiber compressive failure and matrix tensile failure and matrix compressive failure. In this write-up,3DHashin failure criteria in reference[22]wasadopted to trackmatrix and fiber damages as summarizebelow:

Matrix failure in tension $\left(\sigma_{22}+\sigma_{33}>0\right)$

$$D_{mt}=\frac{1}{Y_t^2}\left(\sigma_{22}+\sigma_{33}\right)^2+\frac{1}{S_t^2}\left(\sigma_{23}^2-\sigma_{22}\sigma_{33}\right)+\frac{1}{S^2}\left(\sigma_{12}^2+\sigma_{13}^2\right)=\begin{cases}\geq 1 & failure\\ <1 & no\,failure\end{cases} \quad (1)$$

Matrix failure in compression $\left(\sigma_{22}+\sigma_{33}<0\right)$

$$D_{mc}=\frac{1}{Y_c}\left[\left(\frac{Y_c}{2S_t}\right)^2-1\right]\left(\sigma_{22}+\sigma_{33}\right)+\frac{1}{4S_t^2}\left(\sigma_{22}+\sigma_{33}\right)^2+\frac{1}{S_t^2}\left(\sigma_{23}^2-\sigma_{22}\sigma_{33}\right)+\frac{1}{S^2}\left(\sigma_{12}^2+\sigma_{13}^2\right)=\begin{cases}\geq 1 & failure\\ <1 & no\,failure\end{cases} \quad (2)$$

Fiber failure in tension $\left(\sigma_{11}\geq 0\right)$

$$D_{ft}=\left(\frac{\sigma_{11}^2}{X_t}\right)+\frac{1}{S^2}\left(\sigma_{12}^2+\sigma_{13}^2\right)=\begin{cases}\geq 1 & failure\\ <1 & no\,failure\end{cases} \quad (3)$$

Fiber failure in compression $\left(\sigma_{11}<0\right)$

$$D_{fc}=\left(\frac{\sigma_{11}}{X_c}\right)^2=\begin{cases}\geq 1 & failure\\ <1 & no\,failure\end{cases} \quad (4)$$

where σ_{ij} are the stress components. X_c and X_t denote the fiber strengthsin compression and tension, Y_c and Y_t are the matrix strengths in compression and tension, S and S_t denote allowable shear strengths.

Inter-laminar Damage

Delamination is the main damagemode under large mass impact test, and can be used as a criterion to analyze the impact behavior of composite laminates.With the view to determinethe location and sizeof damage, cohesive interface elements are insertedbetween two sub-plies.Inthis study,cohesive interface elements based onbilinear traction separation law, composed of crack initiationand damagepropagationis adopted.

Damage criterion

The interaction of two adjacent layers in the composite laminate is regardedas inter-laminar behavior and termed as initial linear elastic before delamination occurs. The traction stress at the inter-ply is governed by 3 modes (normal and two shear tractions) described in [23]and expressed by the relation,

$$\begin{bmatrix}N\\ S\\ T\end{bmatrix}=\begin{bmatrix}K_n & 0 & 0\\ 0 & K_s & 0\\ 0 & 0 & K_t\end{bmatrix}\begin{bmatrix}\delta_n\\ \delta_s\\ \delta_t\end{bmatrix} \quad (5)$$

N , S and T are the allowable traction stresses for the three modes, K denotes stiffness of interaction, and δ is the separation displacement.

A quadraticstress interaction criterion is chosen to regulate the delamination damage criterion. With this criterion, damage initiates when quadratic function reacheszero, and presented as follow:

$$\left(\frac{\sigma_n}{N}\right)^2+\left(\frac{\sigma_s}{S}\right)^2+\left(\frac{\sigma_t}{T}\right)^2\geq 1 \quad (6)$$

In Eq. (6) N , S and T represent the interface strengths in the normal and shear directions, respectively, and σ_n , σ_s and σ_t are the corresponding interface stresses.The mixed mode energy based criterionisselected for evolution of damage which defines the variation of the damage factor *d* as indicated below.

$$d = \frac{\delta_m^f \left(\delta_m^{\max} - \delta_m^0\right)}{\left(\delta_m^f - \delta_m^0\right)} \tag{7}$$

$$\delta_m = \sqrt{\delta_n^2 + \delta_{shear}^2} = \sqrt{\delta_n^2 + \delta_s^2 + \delta_t^2} \tag{8}$$

where $\delta_m^{\max}$ refers to the peak value of mixed mode displacement. In Eq. (7) δ_m^f is the complete failure mixed mode displacement and δ_m^0 is the effective crack initiation displacement as described in reference[24]. The δ_m parameter in Eq. (8) corresponds to the normal, sliding and tearing mixed modes.

Damage Evolution

Delamination evolution under mixed mode loading is demonstrated by the 'Power law' as defined in reference[25]:

$$\left(\frac{G_I}{G_{IC}}\right)^{\alpha} + \left(\frac{G_{II}}{G_{IIC}}\right)^{\alpha} + \left(\frac{G_{III}}{G_{IIIC}}\right)^{\alpha} = 1 \tag{9}$$

where G_j and G_{jc} are the energy release and critical energy release rates under the fracture moderespectively; G_{IC} , G_{IIC} and G_{IIIC} are the normal, shear and parallel shear fracture mode energy, with α denoting cohesive property.

FORTRAN pre-compiler code involving these constraint equations is written and executed into the commercial explicit finite element software ABAQUS 6.11 version through a user-coded material subroutine[26].

III. Simulation of Model

GeometryModeling and Boundary Conditions

E-glass fiber/epoxy composite laminate plate of diameter 168 mm and thickness2mm with twoconfigurations $[90_4/0_2/90_4]$ and$[90/45/45/0/-45]_S$ of cross-ply and quasi-isotropic, respectively are developed for impact simulation usingexplicit finite element ABAQUS software. Fixed boundary conditions is fully defined along the edges of the laminated composite plate.The sphere-shaped impactor with radius 10 mm is modeled as an analytical rigid body of mass 1.6 kg as the one used in the empirical set up. A force of magnitude 15.69 N and initial velocity 0.2 m/sare prescribed to the impactor in the transverse direction with all DOFs constrained to zero replicating experimental conditions.

Finite Element Used and Mesh Density

A solid continuum (C3D8R) element and cohesive (COH3D8) formulations are incorporated into the model to simulate inter-laminar damage formation. Each ply in the composite is digitized 8-node elements with 3 DOF for each node and a reduced integration arrangement. The quadratic strain interaction criterion and B-K energy fracture criteria were used to predict delamination damage initiation and propagation, whiles stress-based Hashin failure criterion was chosen for intra-laminar damage. Surface-based cohesive contact model of finite-thickness is employed between plies of different fiber configuration to model delaminationcrack initiation and propagation using

quadratic stress interaction criterion. Failed cohesive elements are permitted to remain in the model to avoid penetration between delamination layers. Coarse mesh of element size (6 mm x 6 mm) is employed outside the impact region where no damage is expected,whiles finer mesh with elements size of 0.8 mm × 0.8 mm is used in the impact area of the composite plate.A total number of 27880 solid and 5576 cohesive elements are adopted in the cross-ply laminate while 27880 solid and 25092 cohesive elements are employed in thequasi-isotropic laminate to stimulate the model. Fig. 1 shows the finite element model of the sphere-shaped impactor and the circular composite laminate plate.

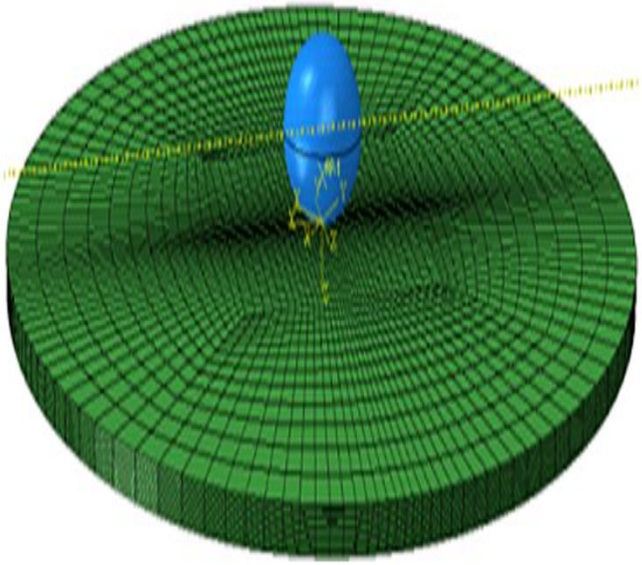

Fig. 1: Finite element model

Contact Algorithm and Material Properties

The interaction between composite laminate plate and impactor is activated by surface-to-surface contact pairs within ABAQUS/Explicit platform which uses penalty enforcement contact method[27]. The 10-layer E-glass composite laminate of two stacking configurations $[90_4/0_2/90_4]$ and $[90/45/45/0/-45]_S$are employed for analysis. The values of material properties [22, 24] and cohesive interface elements [28] are compiled in Table no 1.

Table no 1: Material properties employed in the simulation

Density		2000 kg/m^3
Laminate	Elastic properties	E_{11} = 43.9 GPa; $E_{22} = E_3$ = 15.4 GPa; $\nu_{12} = \nu_{13} = \nu_{23}$ = 0.3;
		$G_{12} = G_{13}$ = 7.0 GPa ; G_{23} = 5.31 GPa
	Strength	X_t=1324 MPa; X_c= 758 MPa; Y_t= 74 MPa; Y_c= 167 MPa;
		S_{12} = 45 MPa; S_{23} = 27 MPa
Cohesive	Elastic properties	$K_n = K_s = K_t = 10^5$ N/mm^3
elements	Strength	N= 30 MPa; S = T= 60 MPa
	Fracture energy	G_n = 0.3 N/mm; $G_s = G_t$ = 0.7 N/mm; a=2

FE Analysis Procedure

The constitutive formulation of each constituent incorporated in CDM is applied into a user-coded material subroutine (VUMAT), available in explicit commercial finite element software ABAQUS inFORTRAN code is

illustrate in the flow chart presented in Fig. 2. During each increment, ABAQUS/Explicit transfers information of the strain increment to subroutine, including the material properties, strain increment of the current increment step, time increment magnitude in addition to the state variables of the previous increment step such as strain and damage. Based on the corresponding constitutive models, the stresses and damage states on the layers and interfaces can be obtained. Once the failure initiation criterion is reached, the stiffness reduction is carried out by updating the damage variables, and then the stresses at the integration points of elements are updated by the reduced stiffness matrix. At last, the updated state variables are returned to ABAQUS to push next increment analysis until the end of the impact process.

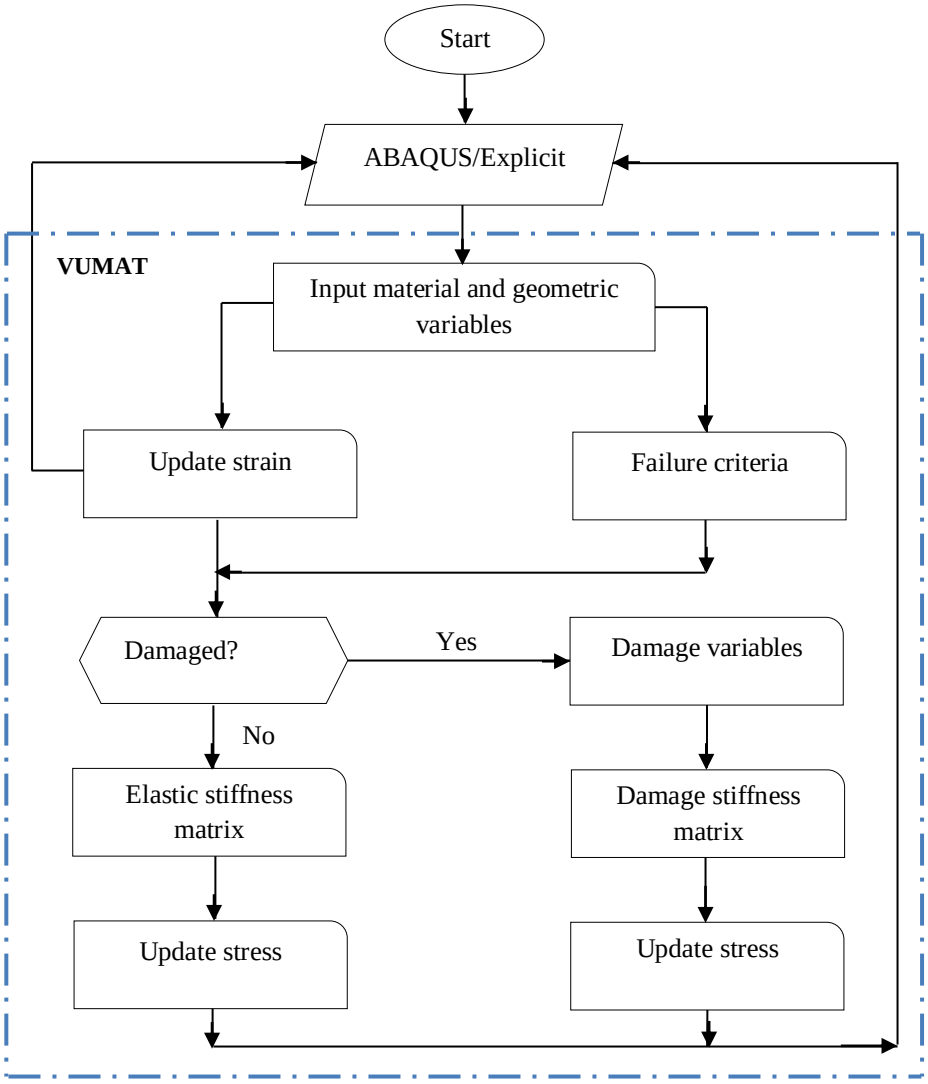

Fig. 2: Flow chart of subroutine (VUMAT)

IV. Results and discussion

Numerical result obtained from the model with initial impact velocity was discussed to validate the model.The impact damage variables such as force and displacement with corresponding impact energy test levels (ranging from 3.14–15.7 J) were compared with experimental test[28].The simulation and experimental comparison with respect to damage size at the impact and bottom surfaces of the quasi-isotropic composite laminate is presented for analysis besides the intra-laminar damage portfolios.

Validation of Study

Numerical result obtained from the cross-ply of stacking sequence $[90_4/0_2/90_4]$ with initial velocity 0.2 m/s was applied to authenticate the applicability of the proposed model. Here, two impact tests were performed. In the first assessment (full model), cohesive interface elements were introduced at each interface irrespective of fiber orientation, thus, interfaces (1-9), while in the second analysis (reduced model), cohesive interface elements were inserted only at the interfaces between plies of different fiber orientation (i.e. interfaces 4 and 6). During the validation, it was observed that damage on the plies of same fiber direction in the former impact test was virtually nonexistent. However, damage was found in the latter impact test on interfaces 4 and 6. When these two damage models interfaces were assessed thoroughly, a reasonable relationship was observed; especially, the reduced model experiences no damage on any of the interfaces as compared to the insignificant damage prediction on the corresponding full model. The extent of matching between the models damage behavior, suggested that the proposed model was consistent and capable for impact behavior analysis. Additionally, numerical simulation and experimental test force as a variable of time and displacement were compared as shown in Figs. 3 and 4. Observably in Fig. 3, simulation results and test data were found to be in better accord with insignificant marginal model variance of 0.06, 3.2 and 3.7 % corresponding to impact energy levels of 3.14 6.28 and 15.7 J, respectively. The discrepancy may arise due to approximation of the failure criteria in the model. In Figs. 3(a-c), maximum impact load of 1277, 1783 and 1786 were predicted for the three ascending energy regimes with corresponding impact energy levels, which agrees excellently with observation test values of 1265, 1841 and 1855 N, respectively. All the impact energy thresholds display comparable responses of quadratic loop curve with load increasing swiftly to maximum during initiation before declines in slope for propagation. The rapid load drop-off shows the maximum limit of residual stress carrying capacity of the composite laminate. The reason may be necessitated by inter-laminar interaction of the layers after degradation of material mechanical properties. This bear witness that the failure criteria adopted in the model to activate stiffness degradation was better approximated to represent experimental arrangement.

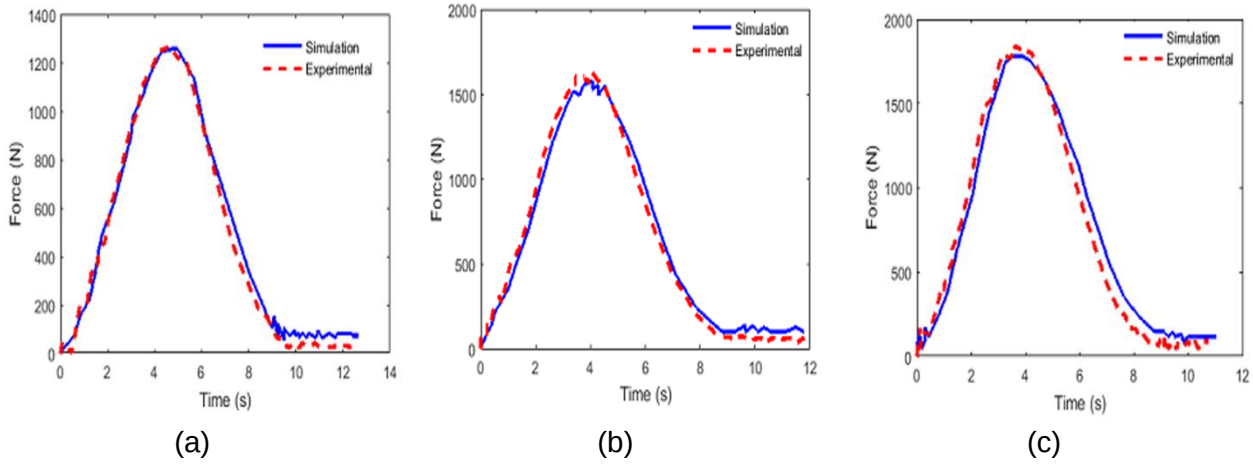

Fig. 3:Impact force-time curves under different impact energy levels (a) 3.14 J (b) 6.28 J (c) 15.7 J

The impact force-time curves were converted into impact force-displacement graphs as displayed in Fig. 4. In the plots of Fig. 4(a-c), same trend of curves for numerical and physical test under the corresponding impact energy regimes were obtained. From the samples, maximum observation force of 1255 N, 1642 N, 1840 N, 1836 N and 1737 N which corresponds to impact energy levels of 3.14, 6.28 and 15.7 J, a reasonable numerical prediction values of 1233 N, 1808 and 1752 N were attained. Once more, this phenomenon most likely arises due to excessive contact pressure between the impactor and composite laminate plate, thus, resulting in matrix cracking and fiber braking as well as debonding of matrix-fiber interface. It was noted however that, all the predictions were in good faith with experimental data except in the 15.7 J impact energy regimes where the experimental curve moved outwards from the predicted result (that is, displacement variance of approximately 49 %). The area under the curve (closed loop) was the absorbed energy which progressively transferred from the spherical impactor to the composite laminate via the ultimate load-carrying threshold. Also, the good match between the numerical simulation and experimental test shows effectiveness in the application of the model to predict structural damage behavior under low mass impact loading condition. The parabolic curve seemly related to damage initiation and progression in the

laminated composite plate. It was evident that the obtained numerical results emphasized the need to incorporate cohesive interface elements in the damage model to track delamination development. The study also showed that load-time histories were similar and consistent for the composite laminate irrespective of the impact energy levels. The threshold load failure was attributed to the bending response as the laminate absorbs impact energy in the form of flexural stresses. Herein, matrix cracking happens alongside fiber damage and delamination propagation envisioned. This contact pressure presumably creates damage due to friction between the impactor and the composite laminate leading to increase in the impact duration. This also confirms that decreasing in the impact load generates higher contact area with shear stresses leading to delamination damage.

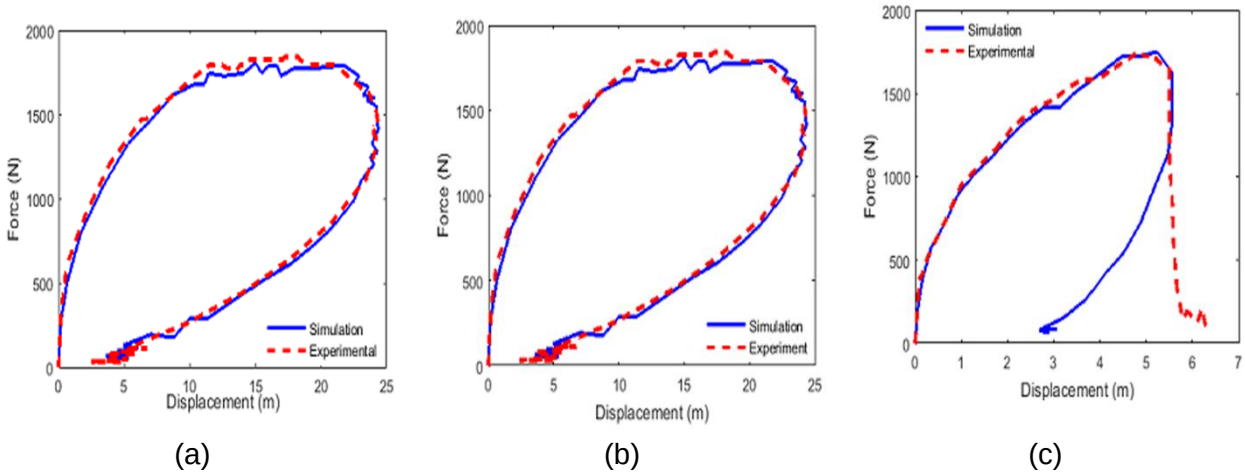

Fig. 4: Impact force-displacement curves for different impact energy levels (a) 3.14 J (b) 6.28 J (c) 15.7 J

Structural Damage Responses

Analysis of intra-laminar damage

Figure 5 compares the predicted and experimental damage area on top and bottom surfaces under three representative impact energy levels (3.14, 6.28 and 15.7 J). With impact energy level of 3.14 J a visible damage occurs on the impact face, while excessive deformation was captured across almost the entire bottom face of the laminated composite plate, which was believed to be matrix cracking in both the simulation and empirical test surfaces. Similar obvious and consistent trend occurs on the impacted face when the impact energy was augmented to 6.28 J; herein, the bottom surface of the composite laminate experienced same severe damage growth for both experimental and simulation prediction. Additionally, the back surface for the numerical prediction suffered excessive wrinkle damage as compared to the experimental event. Finally with impact energy threshold of 15.7 J, complete damage and failure on both faces manifested due to bulging and crumpling of the composite laminate through measured test results. On the contrary, the computational model demonstrated continuous crater with scrunching damage shape on both surfaces for the fiber to break besides matrix cracking, yet, no total perforation emerged. This stiffness phenomenon attested to the capability of the proposed model for impact damage behavior assessment of the composite laminate. In all the impact energy levels considered, the largest matrix damage ensued on the bottommost surfaces causing failure in the form of fiber and matrix as well as fiber-matrix debonding which results in reduction of compressive and tensile strength of the composite laminate. This phenomenon may probably emerge as a result of long contact duration for provocation of the impactor to rebound. The damage discrepancy between the bottom surface and impact surface was significant showing that failure in the composite laminate occurs as a result of excessive elastic deformation, which is in agreement with reference [29]. As expected, the damage modes in composite laminate correspond to matrix tension, matrix compression, fiber tension and fiber compression, however, in this study, the main damage mode predicted was matrix cracking as a result of low impact energy considered.

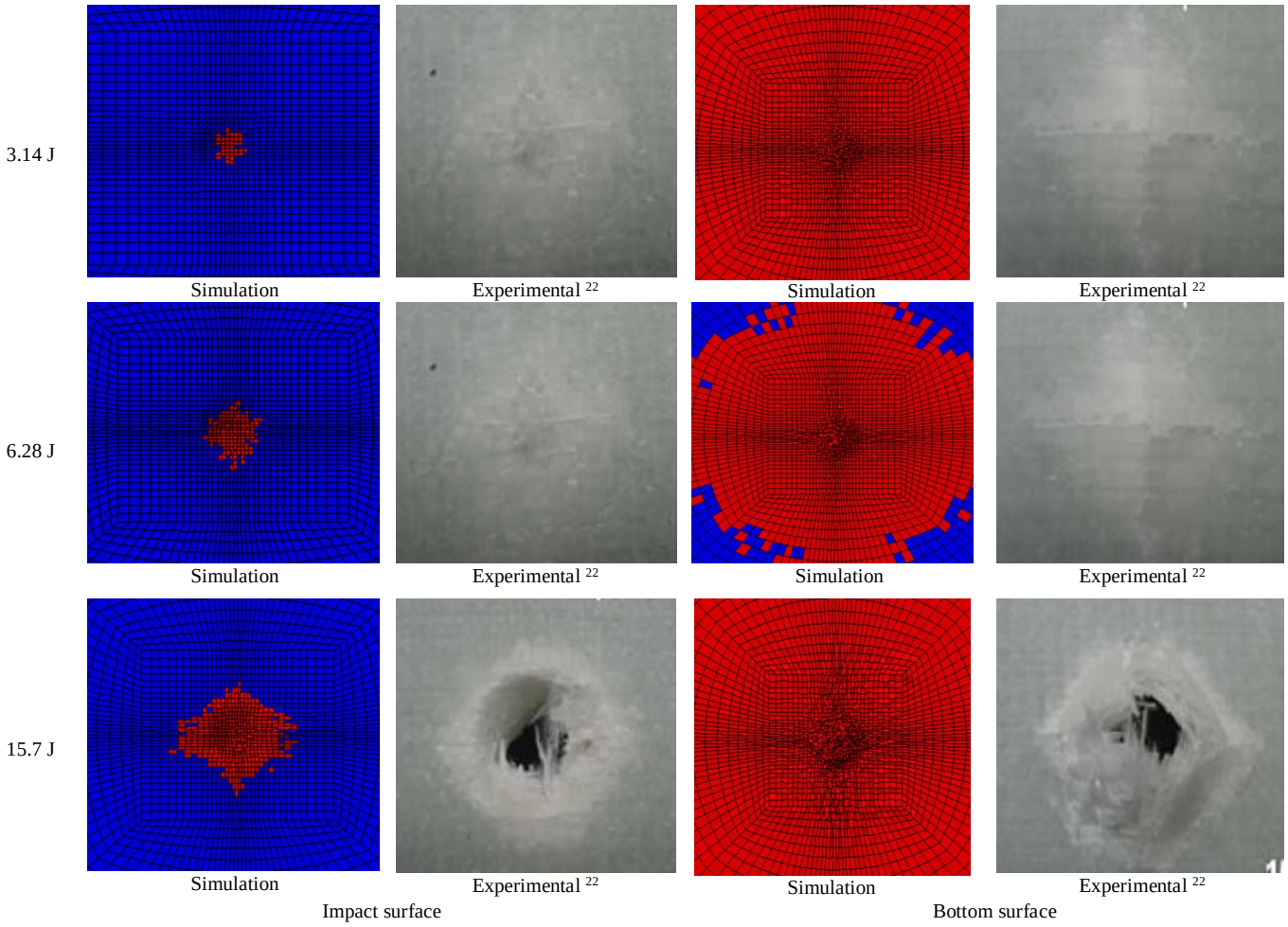

Fig. 5: Simulation and experimental comparison of damage area on impact and bottom surfaces under three impact energy levels

Analysis of inter-laminar damage

Figure 6 shows delamination damage area for each interface on the impacted region under the 15.7 impact energy regime. It can be seen that delamination damage disperses from the impact area towards the circumference of the composite plate. Under this energy threshold, the largest delamination was noted on interface-9 (45/90) near the bottom layer. The smallest delamination area was predicted on the interface-3 (45/0) close to the mid-plane of the composite laminate. Delamination was provoked by the onset of fiber damage which happens concurrently with matrix cracking. Thus, assumed that delamination is the main damage mode in composite laminate which causes substantial degradation in material mechanical properties owing to stress concentration between the inter-laminar plies. This damage is presumed not only triggered by the matrix cracking and fiber breaking but as well as transverse shear stresses. Though, apart from the 9th interface which had the largest delamination, the other interfaces predicted considerable amount of damage which could trigger ultimate failure of the composite structure if disregarded. It was also realized that delamination area propagates with increase in impact energy, and that damage grows as a result of high inter-laminar shear stresses on the impacted area. This state of affair is attributed by long contact duration between the impactor and the bottom layer of the laminated composite plate. Also, it can be attributed to the bending response as the laminate absorbs impact energy in the form of flexural stresses as in Ref. [29].

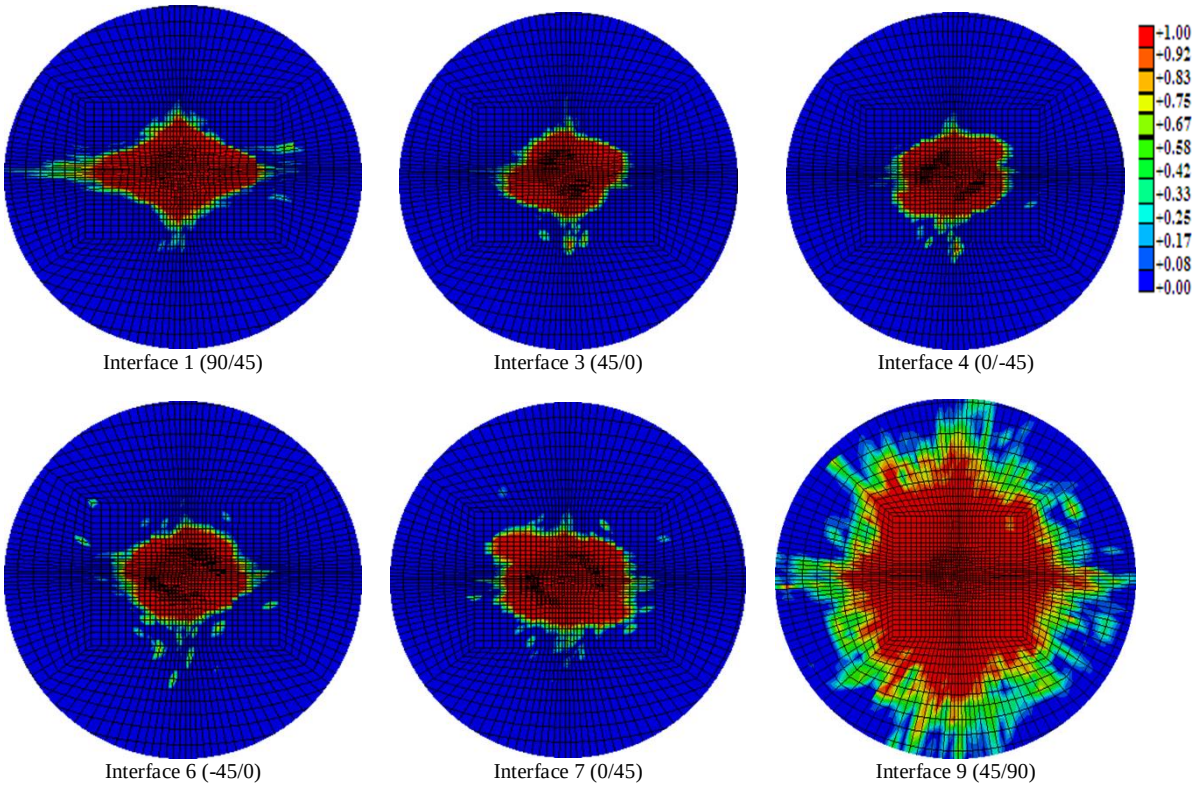

Fig. 6: Delamination damage of typical interfaces subjected to 15.7 J impact energy level

Analysis of stress failure contours

Stress distribution on each layer for impact energy level under 3.14 J is depicted in the graphs of Fig. 7. It can be seen that the largest stress dispersal contour is observed on layer-10 (2178 MPa), followed by the 3rd (45°) and 1st (90°) layers in a reduced threshold. Similarly, stress intensity continues to devastate in the reduced mode from layer 5, 7, 9, 2, 4 and 8, respectively. The smallest stress dispersal trajectory is captured on layer 6 with 396.8 MPa. It can be seen from the numerical analysis that transverse stress triggered quickly on layer-1 matching initiation criterion through layer-10 for delamination of the composite laminate. This sensational development reveals that matrix cracking occurs first leading to delamination. It is also to acknowledge that in all the layers, stress envelop orients towards the stacking configuration direction with spider-shaped pattern. This attests to the fact that laminates stacking sequence have great influence on the extent to which damage dispersed. Also, the variation in stress values may be attributed to contact friction on the composite laminate resulting in local indentation as the impact threshold increases.

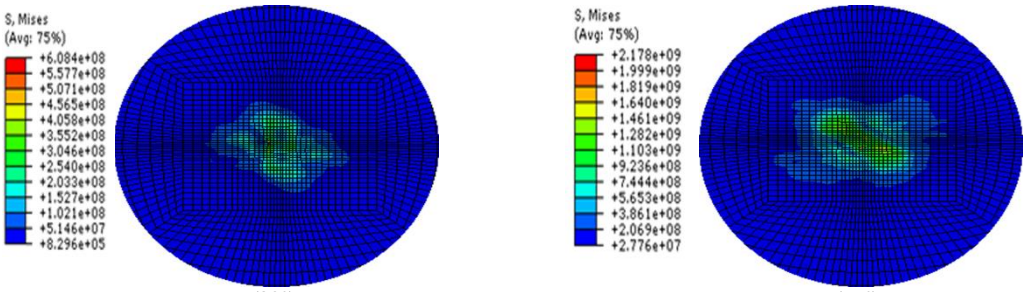

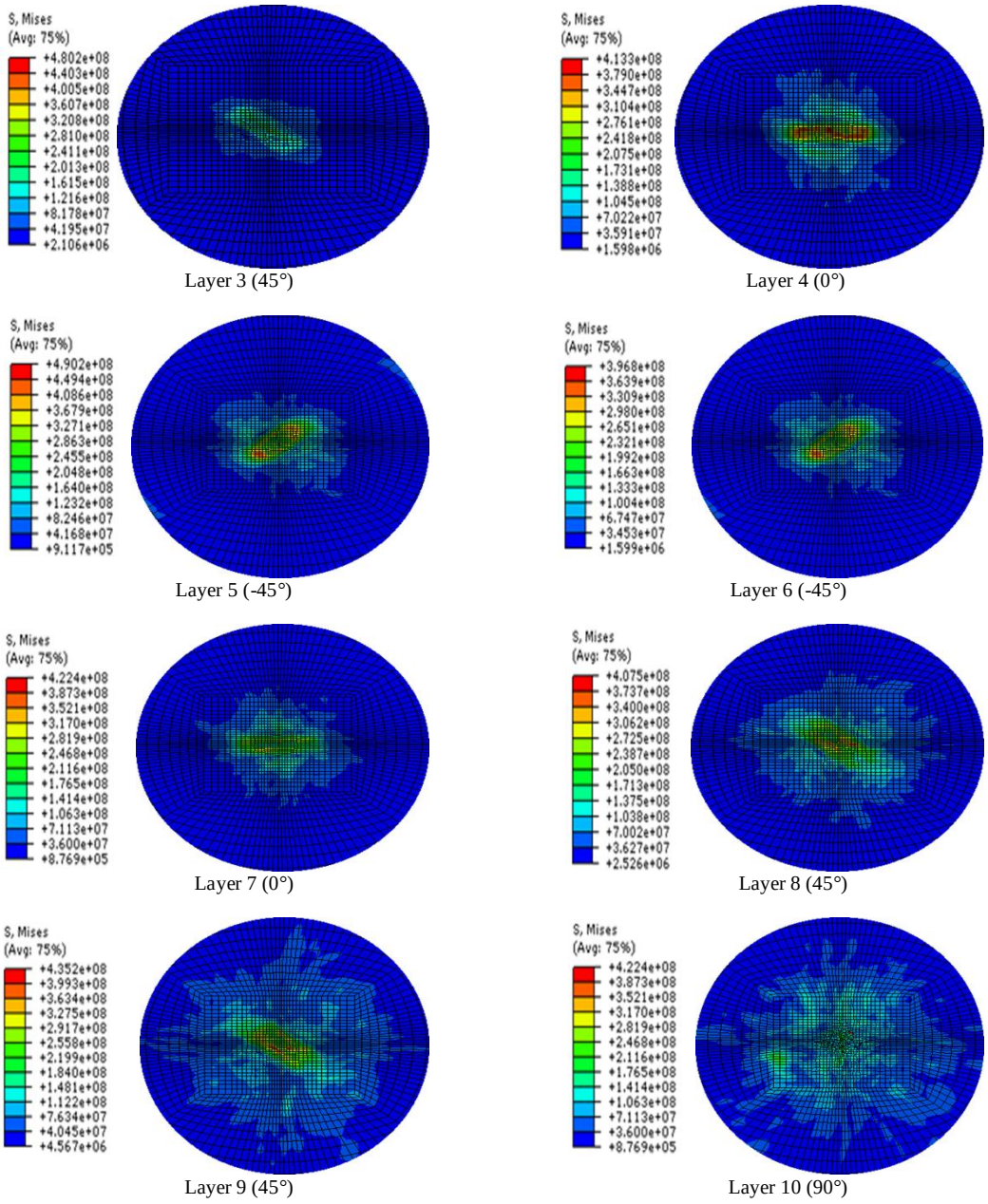

Fig. 7: Stress distribution on each layer under impact energy level of 3.14 J

V. Conclusion

In this study, detailed analysis of a modified damage model was presented and coded in a user-material subroutine VUMAT on ABAQUS/Explicit platform with FORTRAN to trigger damage development and impact characteristics of quasi-isotropic E-glass composite laminate at low velocity. The damage model was compared with experimental data for validation with respect to contact force-time and force-displacement curves. The structural damage responses in terms of intra-laminar failure of the composite laminate were analyzed besides delamination damage and stress failure portfolios, and excellent agreement was achieved between simulation predictions and experimental resultsto verify the efficiency and dependability of the proposed models under low velocity impact

loading conditions.In the simulation model thoughreveals largedeformation,yet,did not yield in total fracture.This shows the importance of cohesive interface element in the model to trigger constraints effect due to impact on the initiation phase. The studyalso reveals that the bottom most surface suffersgargantuandeformationcompare to the impact surface.It divulges that the extent of damage area in each ply of the composite laminate orients in the fiber direction in 'star-shaped contour. Themodel wastherefore found to be capable for structural impact analysis on both cross-ply and quasi-isotropic composite laminate. The current model will be an appropriate tool in future to study damage progression behavior in composite laminates with cluster or multiply lay-ups under large mass impact test.

VI. Acknowledgment

The research is partially supported by the Innovative Foundation for Doctoral Candidate of Jiangsu Province, China (KYLX15_1049) and the Postdoctoral Science Foundation of Jiangsu Province, China (1402101C) during the course of this work.

References

1. Choi I-H, Kim I-G, Ahn S-M, Yeom C-H. Analytical and experimental studies on the low-velocity impact response and damage of composite laminates under in-plane loads with structural damping effects. *Composites Science and Technology.* 2010;70(10):1513-1522.
2. Xiao S, Chen P, Ye Q. Prediction of damage area in laminated composite plates subjected to low velocity impact. *Composites Science and Technology.* 2014;98:51-56.
3. Olsson R. Analytical prediction of large mass impact damage in composite laminates. *Composites Part A: Applied Science and Manufacturing.* 2001;32(9):1207-1215.
4. Hosur MV, Adbullah M, Jeelani S. Studies on the low-velocity impact response of woven hybrid composites. *Composite Structures.* 2005;67(3):253-262.
5. Zhang D, Sun Y, Chen L, Pan N. A comparative study on low-velocity impact response of fabric composite laminates. *Materials & Design.* 2013;50:750-756.
6. Sevkat E, Liaw B, Delale F. Drop-weight impact response of hybrid composites impacted by impactor of various geometries. *Materials & Design.* 2013;52:67-77.
7. Soliman EM, Sheyka MP, Taha MR. Low-velocity impact of thin woven carbon fabric composites incorporating multi-walled carbon nanotubes. *International Journal of Impact Engineering.* 2012;47:39-47.
8. Mitrevski T, Marshall IH, Thomson RS, Jones R. Low-velocity impacts on preloaded GFRP specimens with various impactor shapes. *Composite structures.* 2006;76(3):209-217.
9. Lopes C, Camanho P, Gürdal Z, Maimí P, González E. Low-velocity impact damage on dispersed stacking sequence laminates. Part II: Numerical simulations. *Composites Science and Technology.* 2009;69(7):937-947.
10. Lopes C, Seresta O, Coquet Y, Gürdal Z, Camanho P, Thuis B. Low-velocity impact damage on dispersed stacking sequence laminates. Part I: Experiments. *Composites Science and Technology.* 2009;69(7):926-936.
11. Zhang X, Bianchi F, Liu H. Predicting low-velocity impact damage in composites by a quasi-static load model with cohesive interface elements. *Aeronautical Journal.* 2012;116(1186):1367-1381.
12. Feng D, Aymerich F. Finite element modelling of damage induced by low-velocity impact on composite laminates. *Composite Structures.* 2014;108:161-171.
13. Ghoushji M, Alebrahim R, Zulkifli R, Sulong A, Abdullah S, Azhari C. Crashworthiness characteristics of natural ramie/bio-epoxy composite tubes for energy absorption application. *Iranian Polymer Journal.* 2018:1-13.
14. El-baky MAA. Impact performance of hybrid laminated composites with statistical analysis. *Iranian Polymer Journal.* 2018;27(7):445-459.
15. Zeleniakiene D, Griskevicius P, Norvydas V, Aniskevich A, Zukiene K. Simulation of mechanical behaviour of polychloroprene/versatic acid vinyl ester/methyl methacrylate/2-ethylhexyl acrylate copolymer blend. *Iranian Polymer Journal.* 2018;27(2):97-103.
16. Zeleniakienė D, Griškevičius P, Leišis V, Milašienė D. Numerical investigation of impact behaviour of sandwich fiber reinforced plastic composites. *Mechanics.* 2010;85(5):31-36.
17. Safi S, Zadhoush A, Ahmadi M, Tehrani SPR. Hybrid silane-treated glass fabric/epoxy composites: tensile properties by micromechanical approach. *Iranian Polymer Journal.* 2018;27(1):1-11.
18. Safi S, Zadhoush A, Masoomi M. Effects of chemical surface pretreatment on tensile properties of a single glass fiber and the glass fiber reinforced epoxy composite. *Polymer Composites.* 2016;37(1):91-100.

19. Jang J, Sung M, Han S, Yu W-R. Prediction of delamination of steel-polymer composites using cohesive zone model and peeling tests. *Composite Structures.* 2017;160:118-127.
20. Shi Y, Pinna C, Soutis C. Interface cohesive elements to model matrix crack evolution in composite laminates. *Applied Composite Materials.* 2014;21(1):57-70.
21. Kumar D, Roy R, Kweon J-H, Choi J-h. Numerical Modeling of Combined Matrix Cracking and Delamination in Composite Laminates Using Cohesive Elements. *Applied Composite Materials.* 2015:1-23.
22. Du J, Tie Y, Li C, Zhou X. Numerical and Experimental Study for Damage Characterization of Composite Laminates Subjected to Low-Velocity Impact.*Materials Physics and Mechanics.* 2016;27:195-204.
23. Long S, Yao X, Zhang X. Delamination prediction in composite laminates under low-velocity impact. *Composite Structures.* 2015;132:290-298.
24. Shi Y, Swait T, Soutis C. Modelling damage evolution in composite laminates subjected to low velocity impact. *Composite Structures.* 2012;94(9):2902-2913.
25. Riccio A, Ricchiuto R, Saputo S, et al. Impact behaviour of omega stiffened composite panels. *Progress in Aerospace Sciences.* 2016;81:41-48.
26. Version A. 6.11. User's manual. *Dassault Systemes.* 2011.
27. Manual AUs. Version 6.11. *ABAQUS Inc: Providence, RI, USA.* 2011.
28. Wang P, He R, Chen H, Zhu X, Fang D. A novel predictive model for mechanical behavior of single-lap GFRP composite bolted joint under static and dynamic loading. *Composites Part B: Engineering.* 2015;79:322-330.
29. Reddy TS, Reddy PRS, Madhu V. Response of E-glass/Epoxy and Dyneema® Composite Laminates Subjected to low and High Velocity Impact. *Procedia Engineering.* 2017/01/01 2017;173:278-285.